
ARTIFICIAL
INTELLIGENCE

Recognition of Geomagnetic Storm Based on Neural Network Model Estimates of Dst Indices

A. V. Belov^d, A. D. Gvishiani^{a, b}, V. G. Getmanov^{a, b}, A. A. Kovylyayeva^{a, c},
A. A. Soloviev^{a, b}, V. E. Chinkin^{a, b, *}, V. G. Yanke^d, and I. I. Yashin^{a, c}

^a Geophysical Center, Russian Academy of Sciences, Moscow, Russia

^b Schmidt Institute of Physics of the Earth, Russian Academy of Sciences, Moscow, Russia

^c National Research Nuclear University MEPhI, Moscow, Russia

^d Pushkov Institute of Terrestrial Magnetism, Ionosphere and Radio Wave Propagation, Russian Academy of Sciences, Troitsk, Moscow oblast, Russia

*e-mail: v.chinkin@gcras.ru

Received August 30, 2021; revised September 7, 2021; accepted September 27, 2021

Abstract—A method for recognizing geomagnetic storms based on the neural network (NN) model estimates of Dst indices (disturbance storm time) is proposed; observations from the URAGAN muon hodoscope (MH) and neutron monitors are used. A convolutional NN is applied. A decision-making rule for recognition is implemented. Estimates of the probabilistic characteristics of the recognition of geomagnetic storms are formed. An experimental study of the method confirms its effectiveness. It is shown that joint observations of the hodoscope-monitor system, in comparison with separate observations, increase the probability of correctly recognizing geomagnetic storms.

DOI: 10.1134/S106423072201004X

INTRODUCTION

Geomagnetic disturbances arise due to the impact on the Earth's magnetosphere of plasma formations from solar coronal mass ejections, which are usually interpreted as extreme events of the heliosphere. Geomagnetic storms (GSs) are considered to be geomagnetic disturbances with amplitudes greater than the given one. GSs can cause malfunctions in telephone and radio communication lines, pipelines, and power lines; they can lead to malfunctions in the electronics used in aviation and space systems; and they can have detrimental effects on biosystems. Recognition (presence or absence) of GS is a topical scientific problem.

As is known, geomagnetic activity is usually characterized by geomagnetic indices. One of the most common indices is the Dst index, introduced and described in [1, 2]. This index is determined based on the values of the meridian components of the geomagnetic field strength vector of four equatorial magnetic observatories spaced in longitude; and it is calculated by hourly averaging. Dst indices are measured in nanotesla (nT); for quiet states of the magnetosphere, their values are in the range +20 to –40 nT; for GS, Dst indices take values in the range –50 to –150 nT and, in exceptional cases, go beyond the specified range.

The materials of the article are based on information from the following sources:

(1) an experimental matrix time series from the database of the URAGAN muon hodoscope (MH) [3, 4] on the MEPhI site [5]; the MH observations are proportional to the intensities of muon fluxes depending on the extreme events that occur in the heliosphere;

(2) an experimental scalar time series of the isotropic component function calculated by the global survey method [6, 7] from the world database of neutron monitors (NMs) on the IZMIRAN website [8]; the NM observations are proportional to the intensities of neutron fluxes from extreme events in the heliosphere;

(3) experimental scalar time series of the Dst indices' site, World Data Center of Geomagnetism (WDCG), Kyoto [9, 10].

The solution of GS recognition tasks depends on the type of information sources and mathematical methods used. For example, in [11, 12], special two-dimensional functions of variations of muon fluxes and indicator matrices are proposed for GS recognition based on matrix MH observations.

For problems of recognition and prediction of extreme events in the heliosphere and magnetosphere in solar-terrestrial physics, neural network (NN) technologies are widely used [13, 14]. A number of publications related to NNs differ in the variants of the used information sources and NN structures. These circumstances introduce significant variations in the formulation of problems.

The works [15, 16] devoted to GS predictions are written based on the data on solar wind and the use of NN multilayer perceptrons. In [17] a method is presented that combines recurrent NNs with short-term memory and a Gaussian process model to provide probabilistic predictions of Dst indices; and the necessary NN training is implemented. In [18], using a multilayer feedforward perceptron, the predictions of variations in Dst indices from previous values were investigated for several hours ahead.

Publications [19–22] contain descriptions of methods of restoration, correction, forecasting, and classification of the magnetospheric activity characteristics based on NN technology, taking into account the changing conditions of the weather in space. This approach determines the relationships between the input and output parameters based on the experimental data without building physical models, which can be used for complex geophysical systems. The peculiarity of the described methods is that NNs allow solving the tasks in an automated way using satellite data, magnetic measurements on the Earth's surface, and the results of sounding the ionosphere.

In [23–25] the possibility of forecasting the time series of geomagnetic Dst indices is studied. Predictions are based on the parameters of the solar wind and interplanetary magnetic field, measured in an experiment on an American spacecraft, using NN machine learning methods based on classical perceptrons and recurrent networks.

The above review of publications allows us to make the following conclusions:

the possibilities that could be achieved with the joint use of several information sources—MH and NM observations, as well as Dst indices for GS recognitions—are not considered;

solutions are implemented in which the probability of correct recognition is estimated, and at the same time the necessary allowance for the methodically important probability of false recognition is omitted.

This article proposes a GS recognition method using the developed system of model estimates of Dst indices and the implementation of the decision-taking rule. An approach to the implementation of the method is applied, based on joint observations from MH URAGAN, the world network of neutron monitors, and Dst indices from WDCG using convolutional NN training. The probabilistic characteristics of the recognition of geomagnetic storms are estimated. An experimental study of the method has confirmed its effectiveness. It is shown that joint observations of the hodoscope—monitor system, in comparison with separate observations, increase the probability of correct GS recognition.

The results of this article can be used for a variety of scientific and technical applications, including the following example:

in the event of a possible sudden absence (omission) of Dst indices from the WDCG, GSs can be recognized based on prebuilt models of Dst indices, working based only on MH and NM observations;

when a short-term prediction of a GS is required, which is potentially possible based on extrapolation for MH and NM observations.

1. FORMULATION OF THE GS RECOGNITION PROBLEM

All the variables used in this article were discretized with an hour step in a UTC time scale (coordinated universal time). For the problem under consideration, the Dst indices $Y_D(k)$ were realized in the time interval 01/2002–12/2016; the MH observations $X_M(k)$, in the interval 01/2008–12/2018; and NM observations $X_N(k)$, in the interval 01/2002–12/2018. The time index k determined sampling moments Tk , $T = 1$ h. For Y_D the initial and final time indices took on the values $k_0 = 1$ and $k_{f_0} = 131736$; for X_M the start and end indices were $k_{01} = 52285$ and $k_f = 149016$; and for X_N , $k_{02} = 1$ and $k_f = 149016$. From this it followed that in the time interval 01/2008–12/2016, the variables Y_D , X_M , and X_N were realized; and on the interval 01/2017–12/2018, variables X_M and X_N .

Figure 1 shows examples of graphs of the initial variables $Y_D(k)$, $X_M(k)$, and $X_N(k)$ for the 7-month time interval 01/2011–07/2011. On the abscissa axis, the short bold segments mark the areas where GSs actually occurred. On the chart $Y_D(k)$, it can be seen that the GS events caused a drop in variable Y_D .

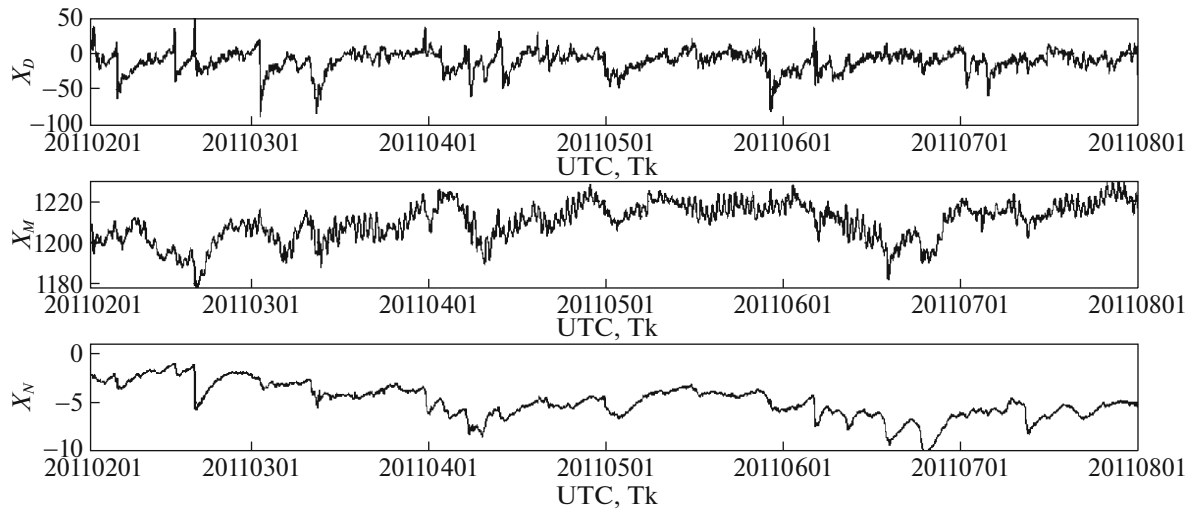


Fig. 1. Graphs of MH and NM observations $X_M(k)$, $X_N(k)$, and Dst indices $Y_D(k)$ with GS plots.

Examination of $Y_D(k)$ in Fig. 1 made it possible to conclude that the average duration of the GS was on the order of 2 to 2.5 days. Analysis of the initial variables made it possible to conclude that for them the average period of additive noninformative low-frequency trends to be filtered was approximately 60–75 days.

Figure 2 contains graphs of variables $Y_D(k)$, $X_M(k)$, and $X_N(k)$ for monthly fragments from 02/2011 to 05/2011 with five GS events, which are marked on the abscissa axes with bold lines in accordance with Fig. 1. The enlarged scale made it possible to analyze in detail the initial variables.

It can be seen from the graphs that the variables $Y_D(k)$ and $X_N(k)$ can be represented as the sum of the informative low-frequency trends and high-frequency noise; and variable $X_M(k)$ is in the form of the sum of an informative low-frequency trend, an interference component from daily fluctuations and high-frequency noise. Analysis of the changes in the informative low-frequency trends of variables $X_M(k)$ and $X_N(k)$ in these figures for monthly intervals allowed us to conclude that their behavior is almost identical over time.

In the practice of analyzing geomagnetic observations, it is generally accepted to make a conclusion about the recognition of GSs according to the criteria that are formed based on the geomagnetic indices. The criterion based on the comparison of Dst indices from the WDCG with a predetermined threshold is quite common and to a certain extent reliable in recognizing GSs. However, in a number of cases, the direct use of Dst indices for recognition may turn out to be problematic due to their possible absence at the current and previous points in time.

We will make the following assumptions:

(1) the current moments of time are given, which correspond to the time indices k satisfying the inequalities $k_{f0} + 1 \leq k \leq k_f$;

(2) the time series of ML observations and NM observations were implemented on the interval with indices $k_{f0} + 1, \dots, k - 1, k$;

(3) the time series of MC observations and Dst indices are implemented on the interval $k_{01} \leq k \leq k_{f0}$; and the time series of NM observations and Dst indices, on the interval $k_{02} \leq k \leq k_{f0}$.

Obviously, the MH observations and NM observations, which are formed based on various physical phenomena and with the help of different measuring devices, contain information about the GS.

It is required to develop a decision-making procedure for GS recognition based on the implemented time series of MH and NM observations for the given current moments of time.

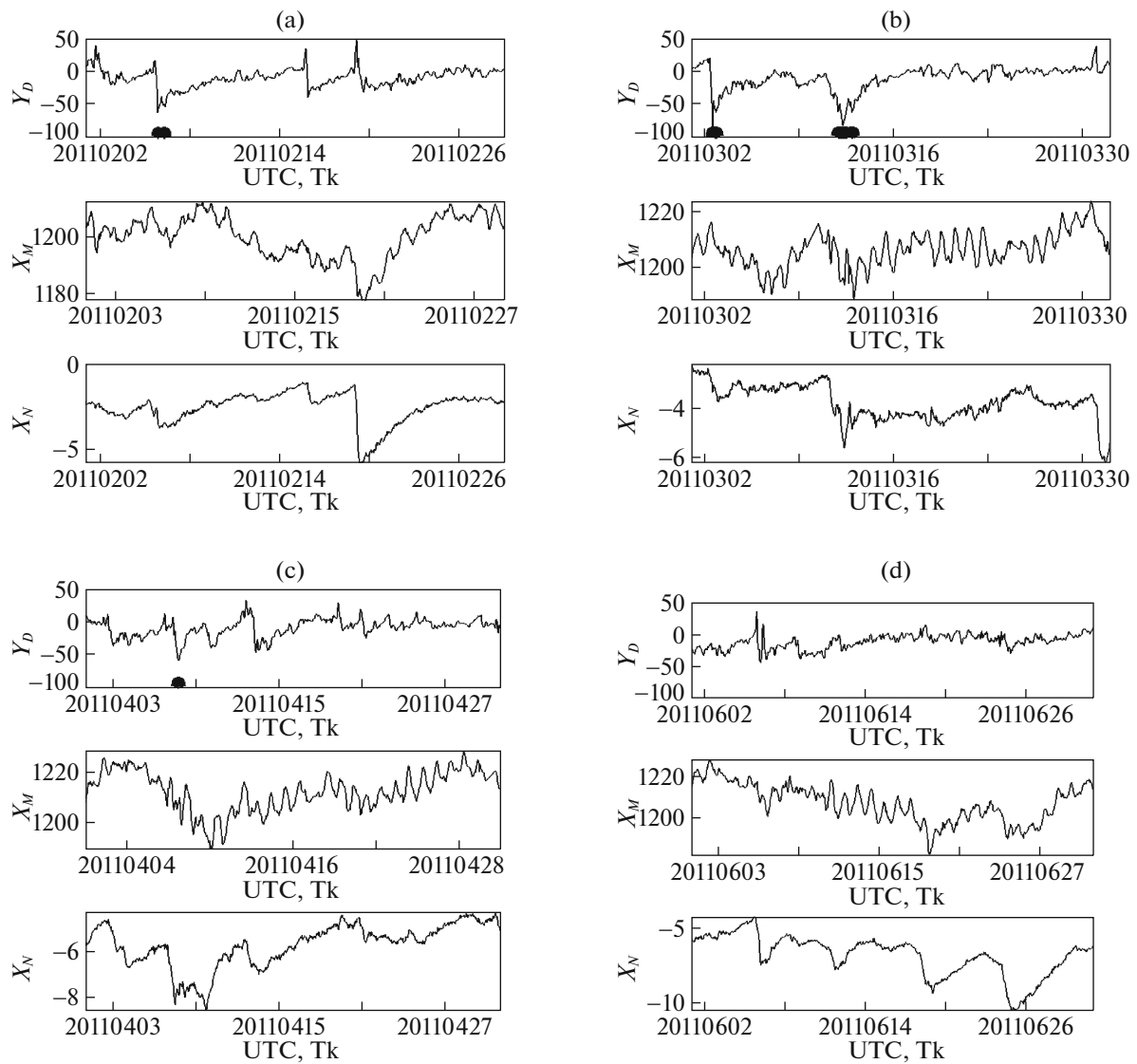


Fig. 2. Graphs of monthly fragments of Dst indices Y_D and MH and NM observations X_M and X_N : (a) 02.2011; (b) 02.2011; (c) 03.2011; (d) 04.2011.

2. GENERAL SCHEME FOR SOLVING THE GS RECOGNITION PROBLEM

The solution of the problem of recognizing a GS here is based on the assumption that the functional relationship between the MH and NM observations, on the one hand, and Dst indices, on the other hand, is distorted by noise. Then, obviously, it is possible to construct a model of Dst indices depending on MH and NM observations based on the corresponding NN.

The general scheme for solving the problem can be divided into four parts:

- procedures for preliminary digital processing of the initial Dst indices, as well as MH and NM observations, for selecting the core informative components in them;

- NN training procedures based on MH and NM observations, as well as Dst indices;

- procedures for calculating the model estimates of Dst indices based on NNs, as well as MH and NM observations;

- the decision-making procedure for GS recognition, which is based on model estimates of Dst indices and their comparison with a predetermined threshold.

Preliminary digital processing procedures are performed for the original Dst indices $Y_D = Y_D(k)$ as well as the MH and NM observations $X_M = X_M(k)$ and $X_N = X_N(k)$. They are filtered to eliminate high-fre-

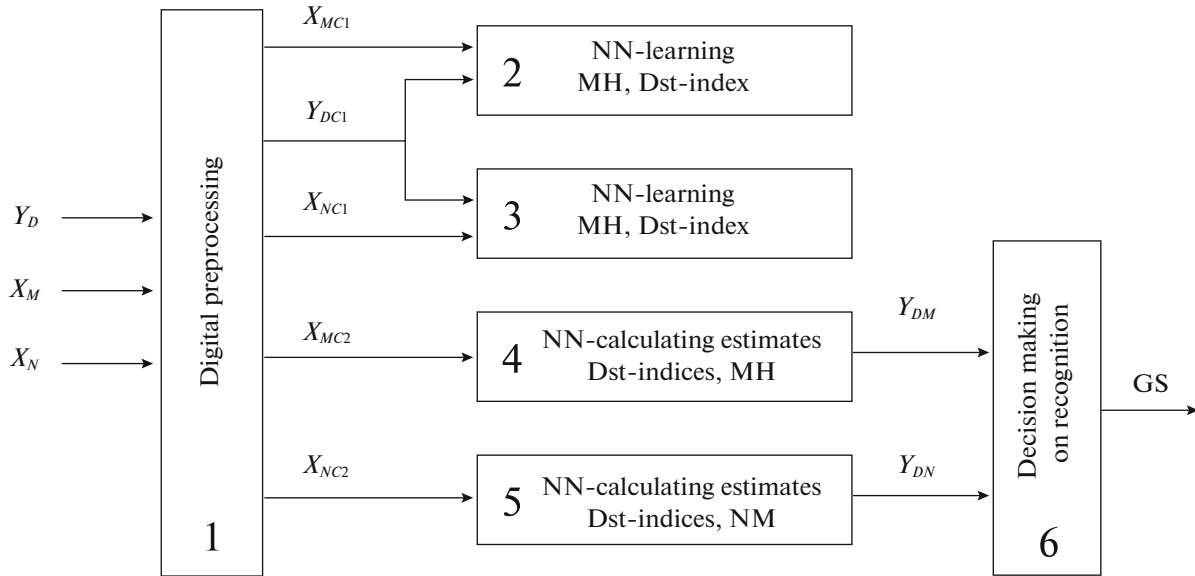


Fig. 3. Scheme of computational operations for solving the GS recognition problem.

quency noise and diurnal fluctuations, and they are scaled to ensure the commensurability of the variables, which is necessary for the efficient operation of the NN. The results of preprocessing procedures for the training stage are denoted as X_{MC1} , X_{NC1} , and Y_{DC1} , for the stage of calculating the model estimates of the Dst indices as X_{MC2} and X_{NC2} .

At the training stage, variables X_{MC1} and X_{NC1} are fed to the input of the MH-NN and NM-NN; the Dst indices Y_{DC1} are used to form target functions in the training functionality; and as a result of training, the NN models are formed. At the stage of calculating the model estimates, the variables X_{MC2} and X_{NC2} , as well as the NN models formed at the training stage, are used.

The decision-making procedure for GS recognition is based on the calculated model estimates of the Dst indices Y_{DM} and Y_{DN} , as well as by comparing them with the set threshold Y_{D0} . The GS solution is implemented using logical calculations.

Figure 3 shows a diagram of the computational operations with the variables indicated above, which explains the solution to the problem under consideration.

The computational operations are subdivided into the following blocks: block no. 1, digital preliminary processing; block nos. 2 and 3, NN training based on MH and NM observations, as well as Dst indices; block nos. 4 and 5, calculations of model estimates of Dst indices based on MH and NM observations; and block no. 6, decision on whether to recognize a GS.

3. STRUCTURE OF CONVOLUTIONAL NN

The results of this article were obtained using a convolutional NN [26, 27]. The use of this network is due to the fact that the initial data and observations were matrix and scalar time series; and convolutional NNs are focused on processing such information. However, it should be noted that the article uses a convolutional NN with a scalar time series and, accordingly, a simplified solution is implemented based on the transformation of the matrix time series of MH observations into a scalar time series by calculating the average values of the matrices of MH observations. The application of a convolutional NN with matrix MH observations will be the subject of further research.

The structure of the used convolutional NN [28] is shown in Fig. 4. We used four convolutional layers (CLs) with an input dimension vector Δk , with dimension convolutional filters Δk_c and activation functions $f(x) = 1, x > 0$ and $f(x) = 0, x \leq 0$. The outputs from the CLs were fed to the input of a fully connected layer (FCL) with the output of dimension $\Delta k_n = 1$.

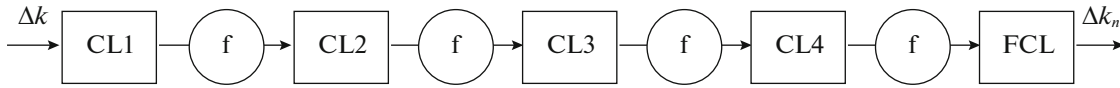


Fig. 4. Convolutional NN structure.

A 9-year interval from 01/2008 to 12/2016 was formed for the MH study; and a 15-year interval, from 01/2002 to 12/2016 for the NM study; the 2-year interval from 01/2017 to 12/2018 was assigned to the calculation of model estimates of the Dst indices Y_{DM} and Y_{DN} .

The work of the NN was based on a system of sliding time windows with a unit step of width Δk , consistent with the average duration of the GS. The training functional was the average over the training interval of the sum of the squares of the differences of the NN models and Dst indices for the rightmost values of the indices of the sliding windows. The introduced functionality was minimized. The NN models obtained as a result of minimization were used to calculate the model estimates of the Dst indices.

Based on the computational experiments, the width of the sliding window $\Delta k = 48$, the dimension of the convolutional filter $\Delta k_c = 8$, and filtering options were determined using the variables defined in Section 1.

4. DECISION-MAKING RULE ON RECOGNIZING GS AND CALCULATING PROBABILITIES OF CORRECT AND FALSE GS RECOGNITION

Let us reduce the GS recognition method to the classification procedure [28, 29] based on the comparison of model estimates of Dst indices $Y_{DM}(k)$ and $Y_{DN}(k)$ with the threshold Y_{D0} . The decision-making rule for GS recognition based on the joint use of MH and NM model estimates of Dst indices for $k_{f0} + \Delta k \leq k \leq k_f$ is that if at least one of the following two inequalities

$$(Y_{DM}(k) \leq Y_{D0}) \quad \text{and/or} \quad (Y_{DN}(k) \leq Y_{D0}) \quad (4.1)$$

holds, then a decision will be taken to recognize the GS: the GS takes place for the time point with index k ; otherwise, the opposite decision will be taken.

Recognition of the GS based on the classification procedure is accompanied by errors: missing correct GS recognitions and formations of false GS recognitions. The errors are determined by the probabilistic characteristics $Y_{DM}(k)$ and $Y_{DN}(k)$. We will use [28] for an approximate calculation of the indicated errors.

Let us form the estimates of errors in which Dst indices $Y_D(k)$, model estimates of Dst indices $Y_{DM}(k)$, and $Y_{DN}(k)$ and the decision-making rule (4.1) for $k_{f0} + \Delta k \leq k \leq k_f$ are used.

We fix the recognition threshold Y_{D0} and consider the moment in time with index k in which the GS takes place: the inequality $Y_D(k) \leq Y_{D0}$ holds. The number of N_{GS} states with the GS, which are determined by the fulfillment of this inequality on the interval $k_{f0} + \Delta k \leq k \leq k_f$ is calculated using the following sum:

$$N_{GS} = \sum_{k=k_{f0}+\Delta k}^{k_f} \text{sign}(Y_{D0} - Y_D(k)), \quad (4.2)$$

where $\text{sign } x = 1, x \geq 0$ and $\text{sign } x = 0, x < 0$. We define $N_{M,GS}$ as the number of correct MH recognitions of the GS using $Y_{DM}(k)$; we find β_M° : an estimation of the probability of correct GS recognition

$$N_{M,GS} = \sum_{k=k_{f0}+\Delta k}^{k_f} \text{sign}(Y_{D0} - Y_D(k))\text{sign}(Y_{D0} - Y_{DM}(k)), \quad \beta_M^\circ = \frac{N_{M,GS}}{N_{GS}}. \quad (4.3)$$

Let us count the number $N_{N,GS}$ of correct NM recognitions of the GS using $Y_{DN}(k)$ and we define the estimate β_N° of the probabilities of correct recognition

$$N_{N,GS} = \sum_{k=k_{f0}+\Delta k}^{k_f} \text{sign}(Y_{D0} - Y_D(k)) \text{sign}(Y_{D0} - Y_{DN}(k)), \quad \beta_N^\circ = \frac{N_{N,GS}}{N_{GS}}. \quad (4.4)$$

The probability score β_{MN}° of the correct recognition of the GS with the combined use of MH and NM observations is found as follows:

$$N_{MN,GS} = \sum_{k=k_{f0}+\Delta k}^{k_f} \text{sign}(Y_{D0} - Y_D(k)) \text{sign}[\text{sign}(Y_{D0} - Y_{DN}(k)) + \text{sign}(Y_{D0} - Y_{DM}(k))], \quad (4.5)$$

$$\beta_{MN}^\circ = \frac{N_{MN,GS}}{N_{GS}}.$$

Quantities N_{0GS} , $N_{M,0GS}$, $N_{N,0GS}$, and $N_{MN,0GS}$ and the corresponding false recognition probabilities of the GS α_M° , α_N° , and α_{MN}° can be calculated by formulas similar to (4.2)–(4.5).

5. EXPERIMENTAL STUDY OF THE GS RECOGNITION METHOD

5.1. Calculation of Estimates of Probabilities of Correct and False Recognition of GS

A time series $Y_D(k)$ of Dst indices was formed on the time interval for calculating the model estimates using the database [9]. Model estimates $Y_{DM}(k)$ and $Y_{DN}(k)$ were calculated. Variables $Y_D(k)$, $Y_{DM}(k)$, and $Y_{DN}(k)$ were compared with the threshold Y_{D0} . The estimates of the probabilities of GS recognition were determined by formulas (4.2)–(4.5) depending on the value of the threshold, which obeyed the inequalities $\bar{Y}_{D01} \leq Y_{D0} \leq \bar{Y}_{D02}$, $\bar{Y}_{D01} = -70$ nT, and $\bar{Y}_{D02} = -20$ nT.

Figures 5a and 5b show graphs of the results of calculating the estimates of the probabilities of false and correct recognition of GS $\alpha_{MN}^\circ(Y_{D0})$ and $\beta_{MN}^\circ(Y_{D0})$ depending on the threshold Y_{D0} ; graphs of the calculations $\alpha_M^\circ(Y_{D0})$, $\beta_M^\circ(Y_{D0})$ and $\alpha_N^\circ(Y_{D0})$, $\beta_N^\circ(Y_{D0})$ have been additionally placed. From Figs. 5a and 5b, it can be concluded that the values of the estimates of the probabilities of correct and false recognition increased with an increase in the threshold, which is quite natural. The graphs show that the limiting fulfillment of the inequality-constraint $\alpha_{MN}^\circ \leq 0.05$ was achieved with $Y_{D0} = -56.2$ nT. In this case, the probability of correct recognition took on the value $\beta_{MN}^\circ = 0.717$; for $\alpha_{MN}^\circ \leq 0.1$, $Y_{D0} = -45.1$ nT and $\beta_{MN}^\circ = 0.823$ were fulfilled. From Fig. 5b, it can be seen that the use of joint observations of the hodoscope-monitor system in comparison with the separate observations increased the probability of correct GS recognition by 10–12%.

5.2. Calculation of Model Estimates of Dst Indices and GS Recognition Results

An experimental study of the GS recognition problem was carried out.

A 4-month interval from August 2018 to November 2018, located outside the boundaries of the training interval, was chosen. Figure 6a shows a plot of the Dst indices $Y_D(k)$ and NN-derived graphs of the calculated model estimates of the Dst indices $Y_{DM}(k)$ and $Y_{DN}(k)$ for $\Delta k = 48$. At the given threshold of $Y_{D0} = -50$ nT, five GS events were realized, which are marked with a “cross in the circle” sign. Reviewing the graph $Y_{DN}(k)$ subject to the threshold $Y_{D01} = -(40..42)$ nT allowed us to establish that there were four instances of correct GS recognitions, marked with a cross in the circle sign, and zero instances of false recognitions of GS.

Reviewing the graph $Y_{DM}(Tk)$ subject to the threshold $Y_{D02} = -(40..42)$ nT showed that two instances of the correct recognition of the GS and one false recognition, marked with a minus sign in the circle, were realized.

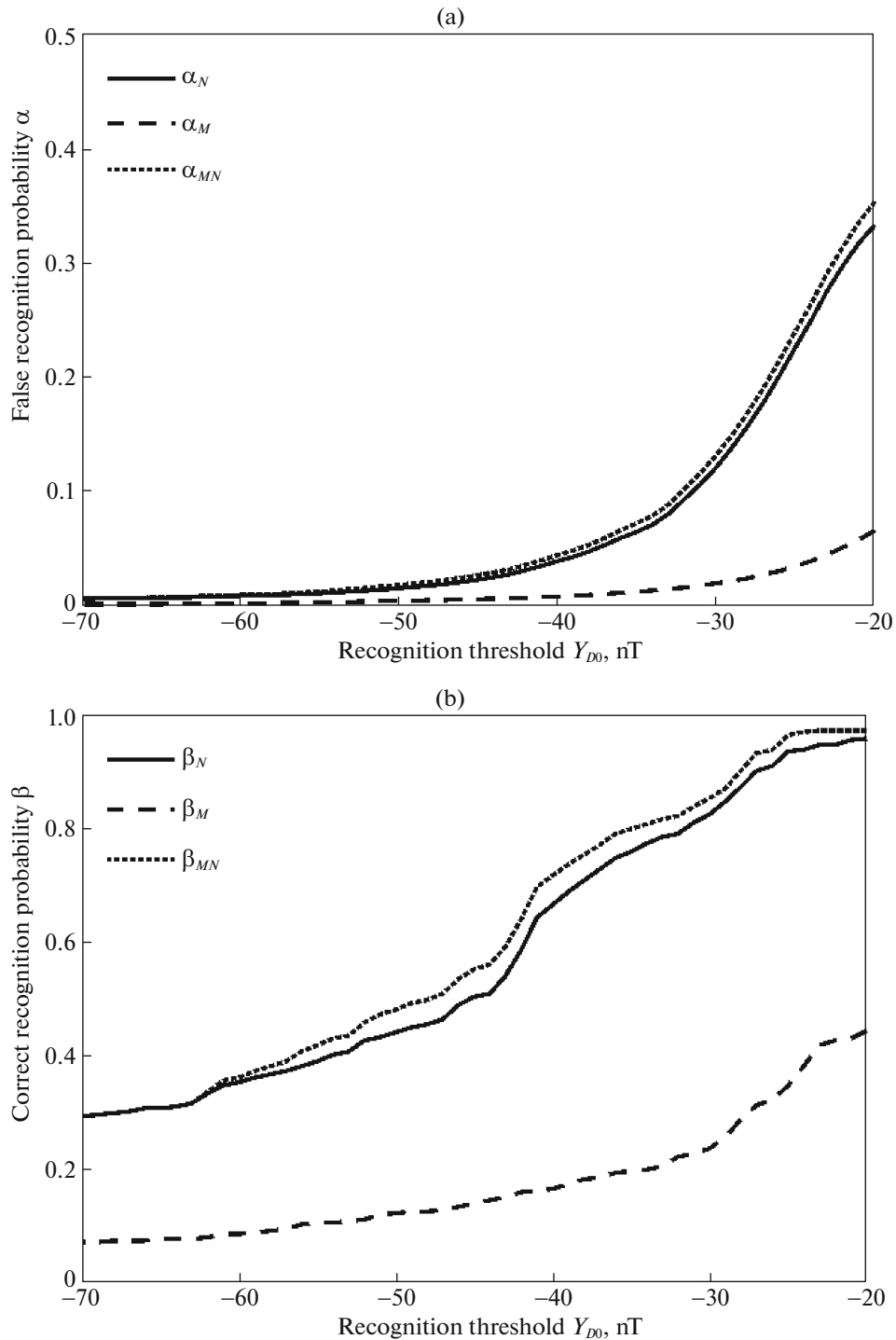


Fig. 5. Graphs of the results of calculating the probabilities of false and correct recognitions depending on Y_{D0} : (a) $\alpha_{MN}^{\circ}(Y_{D0})$, (b) $\beta_{MN}^{\circ}(Y_{D0})$.

The interval from 02/2011 to 05/2011, which was located within the boundaries of the training interval, was chosen. Figure 6b shows a plot of Dst indices $Y_D(k)$ and the NN-derived graphs of the model estimates of the Dst indices $Y_{DM}(k)$ and $Y_{DN}(k)$ for $\Delta k = 48$.

At the given threshold $Y_{D0} = -50$ nT for $Y_D(k)$, seven GS events were implemented. Reviewing the graph $Y_{DN}(k)$ subject to the threshold $Y_{D02} = -(40...42)$ nT allowed us to establish that six correct and two false recognitions of the GS were realized. The graph $Y_{DN}(Tk)$ subject to the threshold $Y_{D02} = -(40...42)$ nT made

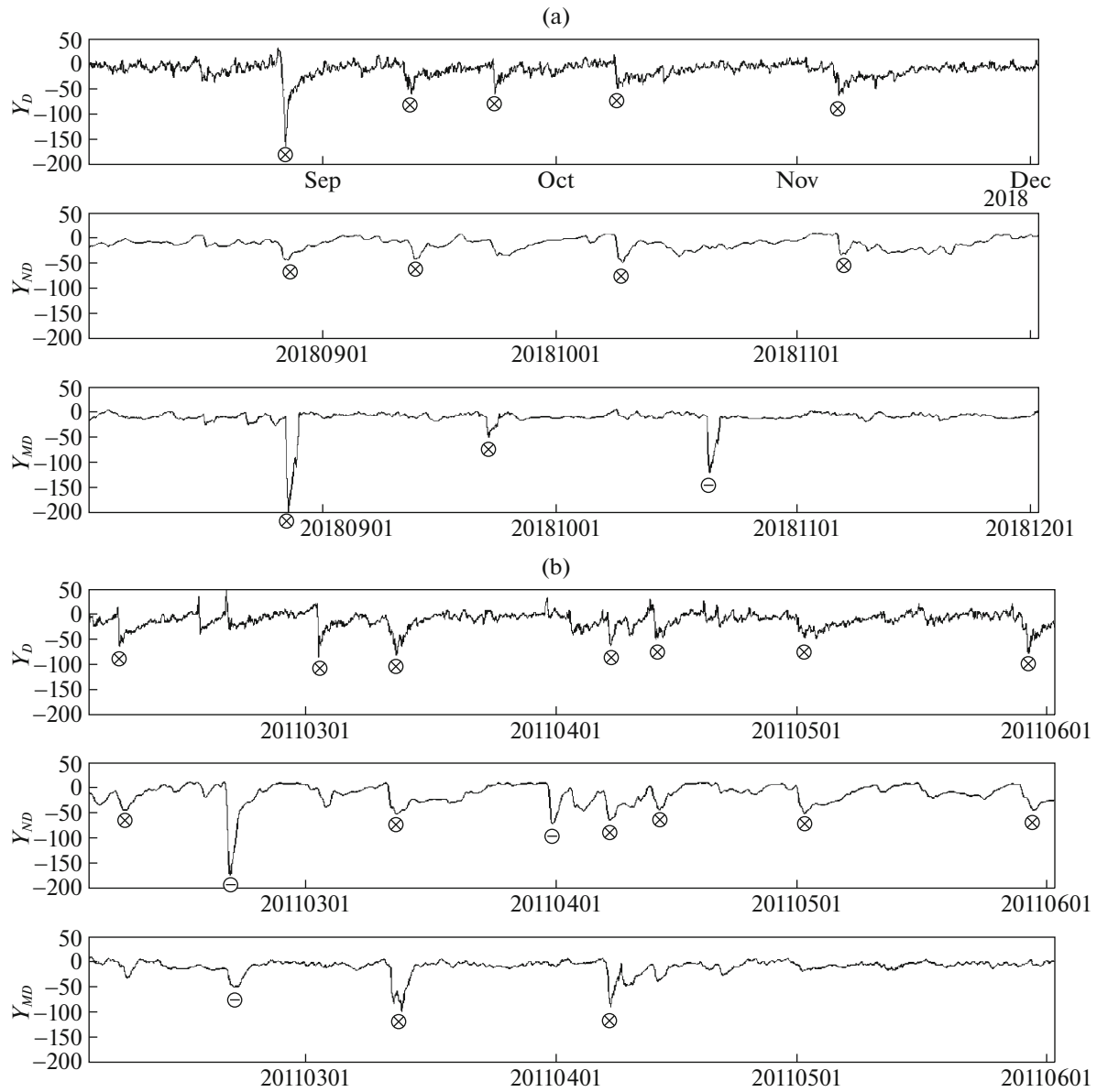


Fig. 6. Dst index plots $Y_D(k)$ and model estimates of Dst indices $Y_{DN}(k)$, $Y_{DM}(k)$: (a) interval from 08/2018 to 11/2018; (b) interval from 02/2011 to 05/2011.

it possible to determine that two correct GS recognitions and one false GS recognition were realized. It can be seen that the variables $Y_{DM}(k)$ and $Y_{DN}(k)$ complement each other when solving the problem of GS recognition.

Calculations were made for NNs with the width of sliding windows $\Delta k = 36, 60$; at the given values of the windows, a decrease in the probability of correct recognition and an increase in the probability of a false recognition were realized.

Analysis of the results of Figs. 5a, 5b, 6a, and 6b led to the conclusion about the reliability of the obtained model estimates of the Dst indices.

5.3. Calculating the Standard Deviations for Differences Y_{DM} , Y_{DN} , and Y_D

The standard deviations were calculated for the differences $\Delta Y_{DM}(k)$ and $\Delta Y_{DN}(k)$ of the model estimates of the Dst indices $Y_{DM}(k)$, $Y_{DN}(k)$ and the original Dst indices $Y_D(k)$,

$$\Delta Y_{DM}(k) = Y_{DM}(k) - Y_D(k), \quad \Delta Y_{DN}(k) = Y_{DN}(k) - Y_D(k),$$

which were taken as indicators of the effectiveness of the proposed GS recognition method. The MH and NM variables were considered on the training intervals and the intervals for calculating model estimates for calm and disturbed GS states.

For MH variables on the training interval, the following sets A_1, A_2 were determined:

$$A_1 = \{k : Y_{DM}(k) \leq Y_{D0}, k_{01} \leq k \leq k_{f0}\}, \quad A_2 = \{k : Y_{DM}(k) > Y_{D0}, k_{01} \leq k \leq k_{f0}\};$$

and N_1, N_2 are the number of indices k for calm and disturbed states:

$$N_1 = \sum_{k \in A_1} \text{sign}(Y_{D0} - Y_{DM}(k)), \quad N_2 = \sum_{k \in A_2} \text{sign}(Y_{DM}(k) - Y_{D0}).$$

Taking into account A_1, A_2, N_1 and N_2 on the training interval, the standard deviations were calculated for calm and disturbed states $\sigma_{DM,S1}$ and $\sigma_{DM,S2}$. Similarly, on the interval for calculating the model estimates of the Dst indices, estimates of the standard deviations were determined for calm and disturbed states $\sigma_{DM,T1}$ and $\sigma_{DM,T2}$. For MH variables, similar formulas were used to calculate the standard deviations.

As a result of the calculations, the following values of the standard deviations were obtained: (1) for MH on the training interval $\sigma_{DM,S1} = 12.47$ and $\sigma_{DM,S2} = 51.45$, on the interval of the calculation of model estimates $\sigma_{DM,T1} = 14.07$ and $\sigma_{DM,T2} = 68.96$; (2) for NM on the training interval $\sigma_{DN,S1} = 17.75$ and $\sigma_{DN,S2} = 63.05$, on the interval for the calculation of model estimates $\sigma_{DN,T1} = 15.55$ and $\sigma_{DN,T2} = 44.57$. The calculation results of the standard deviations allowed us to draw the following conclusions: (1) The MH and NM information sources are practically equal in terms of their characteristics of the standard deviations; (2) estimates of the standard deviations for Y_{DM} and Y_{DN} can serve as indicators of calm and disturbed states when recognizing GSs.

CONCLUSIONS

In this article, a method for GS recognition is proposed based on NN-model estimates of Dst indices obtained using MH and NM observations using convolutional NNs. A decision-making procedure for GS recognition has been developed. A study of the GS recognition method on experimental Dst indices, as well as MH and NM observations for 2002–2018 and 2008–2018, demonstrated its efficiency and effectiveness.

The results of the calculations made it possible to draw a conclusion about the reliability of the obtained model estimates of the Dst indices. The combined use of MH and NM observations showed that the estimates of the probabilities of correct and false recognition were the values $\beta_{MN}^{\circ} = 0.823$ and $\alpha_{MN}^{\circ} = 0.1$. The use of joint observations of the hodoscope–monitor system, in comparison with the use of separate observations, increased the probability of the correct recognition of geomagnetic storms by 10–12%.

The proposed GS recognition method has significant room for improvement, in particular, for the further optimization of its parameters in order to improve the probabilistic characteristics and its adaptation to solve the problem of short-term forecasting of GSs based on the extrapolation of MH and NM observations, as well as promising prospects for use in applied problems.

FUNDING

This study was supported by the Russian Science Foundation (grant no. 17-17-01215-Π).

REFERENCES

1. M. Suigiura, “Hourly values of equatorial dst for the IGY,” Ann. Int. Geophys. Year **35**, 9–45 (1964).
2. M. Suigiura and T. Kamei, “Equatorial Dst-index 1957–1986,” IAGA Bull., No. 40, 14–21 (1991).
3. I. I. Yashin, I. I. Astapov, N. S. Barbashina, et al., “Real-time data of muon hodoscope URAGAN,” Adv. Space Res. **56**, 2693–2705 (2015).
4. N. S. Barbashina, R. P. Kokoulin, K. G. Kompaniets, G. Mannocchi, A. A. Petrukhin, D. A. Timashkov, O. Saavedra, G. Trincherro, D. V. Chernov, V. V. Shutenko, and I. I. Yashin, “The URAGAN wide-aperture large-area muon hodoscope,” Instrum. Exp. Tech. **51**, 180–186 (2008).
5. Data Base of Muon Hodoscope MEPHI. <http://www.nevod.mephi.ru/>.

6. L. I. Dorman, *Cosmic Rays in the Earth's Atmosphere and Underground* (Springer, 2010).
7. A. V. Belov, E. A. Eroshenko, V. G. Yanke, V. A. Oleneva, M. A. Abunina, and A. A. Abunin, "Global survey method for the world network of neutron monitors," *Geomagn. Aeron.* **58**, 356 (2018).
<https://doi.org/10.1134/S0016793218030039>
8. Database of Moscow Neuron Monitor. <http://cr0.izmiran.rssi.ru/>.
9. World Data Center of Geomagnetism, Kyoto. <http://wdc.kugi.kyoto-u.ac.jp>.
10. N. A. Zabolotskaya, *Geomagnetic Activity Indices: A Reference Guide* (LKI, Moscow, 2007) [in Russian].
11. V. E. Chinkin, I. I. Astapov, A. D. Gvishiani, V. G. Getmanov, A. N. Dmitrieva, M. N. Dobrovolsky, A. A. Kovilyaeva, R. V. Sidorov, A. A. Soloviev, and I. I. Yashin, "Method for the identification of heliospheric anomalies based on the functions of the characteristic deviations for the observation matrices of the muon hodoscope," *Phys. At. Nucl.* **82**, 924 (2019).
12. M. N. Dobrovolsky, I. I. Astapov, N. S. Barbashina, A. D. Gvishiani, V. G. Getmanov, A. N. Dmitrieva, A. A. Kovilyaeva, D. V. Peregoudov, A. A. Petrukhin, R. V. Sidorov, A. A. Soloviev, V. V. Shutenko, and I. I. Yashin, "A way of detecting local muon-flux anisotropies with the matrix-form data of the URAGAN hodoscope," *Bull. Russ. Acad. Sci.: Phys.* **83**, 647 (2019).
13. N. A. Barkhatov, *Artificial Neural Networks in Solar-Terrestrial Physics Problems* (Povolzh'e, Nizh. Novgorod, 2010) [in Russian].
14. N. A. Barkhatov and S. E. Revunov, *Heliogeophysical Applications of Modern Digital Data Processing Methods* (FLINTA, Nizh. Novgorod, 2017) [in Russian].
15. H. Lundstedt, "Geomagnetic storm predictions from solar wind data with the use of dynamic neural networks," *J. Geophys. Res.* **102** (A7), 14.255–14.268 (1997).
16. G. Pallochia, E. Amota, G. Consoliniet, et al., "Geomagnetics Dst index forecast based on IMF data only," *Ann. Geophys.* **24**, 989–999 (2006).
17. M. A. Gruet, M. Chandorkar, A. Sicard, and E. Camporeale, "Multiplehour-ahead forecast of the Dst index using a combination of long short-term memory neural network and gaussian process," *Space Weather* **16** (2018).
<https://doi.org/10.1029/2018SW001898>
18. M. V. Stepanova and P. Perez, "Autoprediction of Dst-index using neural network techniques and relationship to the auroral geomagnetics indices," *Geofis. Int.* **39**, 143–146 (2000).
19. N. A. Barkhatov, A. V. Korolev, S. M. Ponomarev, et al., "Long-term forecasting of solar activity indices using neural networks," *Radiophys. Quantum Electron.* **44**, 742–749 (2001).
20. N. A. Barkhatov, N. S. Bellyustin, A. E. Levitin, and S. Yu. Sakharov, "Comparison of efficiency of artificial neural networks for forecasting the geomagnetic activity index Dst," *Radiophys. Quantum Electron.* **43**, 347 (2000).
21. N. A. Barkhatov, A. E. Levitin, and S. Yu. Sakharov, "The method of artificial neuron networks as a procedure for reconstructing gapsin records of individual magnetic observatories from the data of other stations," *Geomagn. Aeron.* **42**, 184 (2002).
22. N. A. Barkhatov, A. E. Levitin, and G. A. Ryabkova, "Artificial neural networks for predicting the indices of geomagnetic activity based on the parameters of the near-Earth space," *Soln.-Zemn. Fiz.*, No. 2 (115), 104–106 (2002).
23. A. O. Efitorov, I. N. Myagkova, V. R. Shirokii, and S. A. Dolenko, "The prediction of the Dst-index based on machine learning methods," *Cosmic Res.* **56**, 434 (2018).
24. S. A. Dolenko, Yu. V. Orlov, I. G. Persianinov, and Ju. S. Shugai, "Neural network algorithm for events forecasting and its application to space physics data," *Let. Notes Comput. Sci.* **3697**, 527–532 (2005).
25. V. R. Shirokii, "Comparison of neural network models for predicting the geomagnetic Dst index on different datasets and comparing methods for assessing the quality of the models," in *Proceedings of the 17th All-Russia Conference Neuroinformatics-2015 with International Participation* (NIYaU MIFI, Moscow, 2015), Part 2, pp. 51–60.
26. Deep Learning Matlab Toolbox. <http://matlab.exponenta.ru>.
27. C. M. Bishop, *Pattern Recognition and Machine Learning* (Springer, 2006).
28. I. Goodfellow, Y. Bengia, and A. Courville, *Deep Learning* (MIT, London, 2016).
29. A. B. Merkov, *Pattern Recognition: Building and Training Probabilistic Models* (Stereotip, Moscow, 2020) [in Russian].